

Low energy properties of SU(2) gauge theory with $N_f = 3/2$ flavours of adjoint fermions

Georg Bergner

*University of Jena, Institute for Theoretical Physics
Max-Wien-Platz 1, D-07743 Jena, Germany
E-mail: georg.bergner@uni-jena.de*

Pietro Giudice, Gernot Münster, Philipp Scior
*University of Münster, Institute for Theoretical Physics
Wilhelm-Klemm-Str. 9, D-48149 Münster, Germany
E-mail: {p.giudice,munsteg,scior}@uni-muenster.de*

Istvan Montvay

*Deutsches Elektronen-Synchrotron DESY
Notkestr. 85, D-22607 Hamburg, Germany
E-mail: montvay@mail.desy.de*

Stefano Piemonte

*University of Regensburg, Institute for Theoretical Physics
Universitätsstr. 31, D-93040 Regensburg, Germany
E-mail: stefano.piemonte@ur.de*

December 12, 2017

Abstract: In this work we present the results of a numerical investigation of SU(2) gauge theory with $N_f = 3/2$ flavours of fermions, corresponding to 3 Majorana fermions, which transform in the adjoint representation of the gauge group. At two values of the gauge coupling, the masses of bound states are considered as a function of the fundamental fermion mass, represented by the PCAC quark mass. The scaling of bound states masses indicates an infrared conformal behaviour of the theory. We obtain estimates for the fixed-point value of the mass anomalous dimension γ^* from the scaling of masses and from the scaling of the mode number of the Wilson-Dirac operator. The difference of the estimates at the two gauge couplings should be due to scaling violations and lattice spacing effects. The more reliable estimate at the smaller gauge coupling is $\gamma^* \approx 0.38(2)$.

1 Introduction

The long and short distance behaviour of QCD-like theories depends significantly on the number N_f of fermion flavours and on the representation of the gauge group under which the fermions transform. For sufficiently small N_f the β -function is negative and the well-known scenario with confinement and asymptotic freedom occurs. However, for large N_f above a certain limit N_f^u asymptotic freedom is lost, the β -function is positive and has an infrared fixed point at the origin. The theory then has a scaling behaviour like ϕ^4 -theory and is non-interacting in the continuum limit. Between these two cases different interesting scenarios are expected. For N_f below the triviality limit N_f^u , the perturbative β -function to two or three loops shows asymptotic freedom near the origin, but develops an infrared fixed point, called Banks-Zaks fixed point, at a finite value of the coupling [1]. If N_f is just below N_f^u , this fixed point is at weak couplings, and the scaling behaviour can be obtained perturbatively. The theory is asymptotically free at short distances, and shows conformal behaviour at large distances, i. e. it is infrared conformal. For smaller N_f the IR-fixed point moves towards stronger couplings, such that perturbation theory ceases to be reliable. Finally, decreasing N_f further below a certain value N_f^l , the IR-fixed point will disappear and the QCD scenario sets in. The region between N_f^u and N_f^l is the *conformal window*. Its upper edge can be estimated perturbatively, but the determination of its lower edge is a non-perturbative problem.

For a theory with N_f below, but near to N_f^l , the β -function is always negative, but might approach zero near a certain finite value of the coupling, see Fig. 1. In this case the coupling will not run, but evolve rather slowly in a certain range of distances or momenta, respectively. Such a behaviour is called *walking*, and in the walking regime the theory behaves approximately conformal [2].

For a given theory, the question to which of these scenarios it belongs, is of fundamental importance for its characteristic features. Based on the perturbative β -function and approximate solutions of the Schwinger-Dyson equations, Dietrich and Sannino [3] have mapped out the phase diagram for non-supersymmetric theories with fermions in different representations of the gauge group SU(N) as a function of N and N_f . It turns

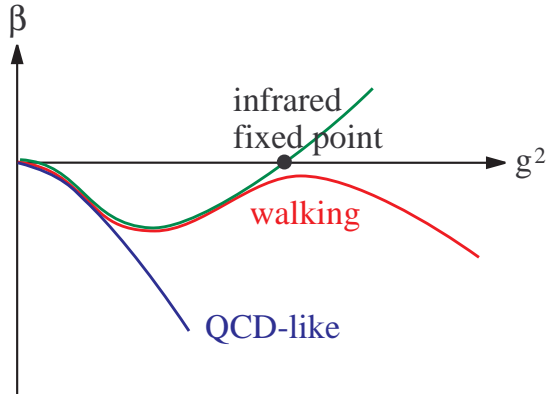


Figure 1: Sketch of the β -functions for QCD-like, conformal, and walking scenarios.

out that for representations higher than the fundamental one, the boundaries of the conformal window are expected to be at rather small values of N_f . In particular, for the adjoint representation they might be near $N_f = 1$ and 2 . To locate their true values requires, however, non-perturbative methods. Therefore, in recent years the scaling behaviour of various theories has been investigated by means of Monte Carlo simulations in the framework of lattice gauge theory.

$SU(N)$ gauge theory with fermions in the adjoint representation has been studied for $N_f = 2$ by various collaborations and appears to be IR-conformal, see e. g. [4] and [5, 6] for reviews. A study of $SU(2)$ with $N_f = 1$ fermion flavours [7] gives indications for IR-conformal behaviour, too. The case of $N_f = 1/2$ describes one flavour of Majorana fermions and corresponds to $\mathcal{N} = 1$ supersymmetric Yang-Mills theory, which has been studied by our collaboration, see [8] and references therein. This theory is QCD-like concerning its scaling behaviour.

It is the purpose of this article to present results about $SU(2)$ gauge theory with $N_f = 3/2$ flavours of fermions in the adjoint representation of the gauge group, where $3/2$ means 3 flavours of Majorana (or Weyl) fermions. Preliminary results have been presented in [9]. We have investigated the masses of various particles, including mesons, glueballs and spin $1/2$ fermion-gluon bound states, the string tension, and the mass anomalous dimension, in order to gain insights into the IR behaviour of the theory.

2 Gauge theory with adjoint fermions on the lattice

We consider $SU(2)$ gauge theory coupled to fermions transforming under the adjoint representation of the gauge group. In the continuum the covariant derivative acting on a fermion field

$$\psi(x) = \psi^a(x)T^a, \quad (1)$$

where $T^a = \sigma^a/2$, $a = 1, 2, 3$, are the generators of $SU(2)$, is given by

$$\mathcal{D}_\mu \psi(x) = (\partial_\mu \psi(x) + ig[A_\mu(x), \psi(x)]), \quad (2)$$

with the gauge field $A_\mu(x) = A_\mu^a(x) T^a$.

The lattice formulation of the theory that we use employs the Wilson gauge action built from the plaquette variables U_p and the Wilson-Dirac operator in the adjoint representation. The lattice action is

$$\mathcal{S}_L = \beta \sum_p \left(1 - \frac{1}{2} \text{tr} U_p\right) + \sum_{xy,f} \bar{\psi}_x^f (D_w)_{xy} \psi_y^f, \quad (3)$$

where D_w is the Wilson-Dirac operator

$$(D_w)_{x,a,\alpha;y,b,\beta} = \delta_{xy} \delta_{a,b} \delta_{\alpha,\beta} - \kappa \sum_{\mu=1}^4 \left[(1 - \gamma_\mu)_{\alpha,\beta} (V_\mu(x))_{ab} \delta_{x+\mu,y} + (1 + \gamma_\mu)_{\alpha,\beta} (V_\mu^\dagger(x - \mu))_{ab} \delta_{x-\mu,y} \right]. \quad (4)$$

Here $\beta = 1/g^2$ is the inverse bare gauge coupling, and the hopping parameter κ is related to the bare fermion mass via $\kappa = 1/(2m_0 + 8)$. The link variables $U_\mu(x)$ are in the fundamental representation of the gauge group $SU(2)$. The gauge field variables $V_\mu(x)$ in the adjoint representation are given by $[V_\mu(x)]^{ab} = 2 \text{tr}[U_\mu^\dagger(x) T^a U_\mu(x) T^b]$.

The lattice extension in all spatial directions is denoted by the number N_s of lattice points. In our simulations the extension in the temporal direction is always given by $N_t = 2N_s$.

The number of fermion flavours is conventionally counted in terms of Dirac fermions. Majorana fermions, satisfying the Majorana condition

$$\bar{\psi} = \psi^T C, \quad (5)$$

where C is the charge conjugation matrix, possess half the number of degrees of freedom as Dirac fermions and are counted as $N_f = 1/2$. Consequently $N_f = 3/2$ is to be interpreted as 3 species of Majorana fermions. In this case the index f in the lattice action counts Majorana fermions and runs from 1 to 3.

In order to reduce lattice artefacts we use in our simulations an improved version of the lattice action with a tree-level Symanzik improved gauge action and stout smearing for the link fields in the Wilson-Dirac operator [10]. The stout smearing is iterated three times with the smearing parameter $\rho = 0.12$.

For Majorana fermions the fermion integration

$$\int [d\psi] e^{-\frac{1}{2} \bar{\psi} D_w \psi} = \text{Pf}(C D_w) = \pm \sqrt{\det D_w} \quad (6)$$

yields the Pfaffian of the Wilson-Dirac matrix. With 3 Majorana fermion fields the functional integrals contain a factor $(\det D_w)^{3/2}$, which can be treated with the PHMC

algorithm. The possible sign of $\text{Pf}(CD_w)$ has to be taken into account in the observables by reweighting. In simulations not too close to the critical hopping parameter κ_c , negative signs are very rare and it was not necessary to consider them in the parameter regions of our simulations for the determination of the masses.

In order to check the possible presence of a negative sign we have generated two runs at the critical parameters corresponding to $m_{\text{PCAC}} \approx 0$ (runs R1 and R3, see Table 1). The eigenvalue distribution for these runs does not completely match the bounds of the polynomial approximation, but they can still be used to check the general properties of the sign problem in this theory without determining the otherwise necessary correction factors on the configurations. We observe that even at these critical parameters no negative sign is obtained for the measured configurations and a gap in the imaginary part Wilson-Dirac eigenvalues around zero appears. The general features of the spectrum scale with the volume (see Fig. 2). Consequently the rather large finite size effects in these runs are most likely preventing a fluctuating Pfaffian sign in this theory. We did not observe such an effect in supersymmetric Yang-Mills theory.

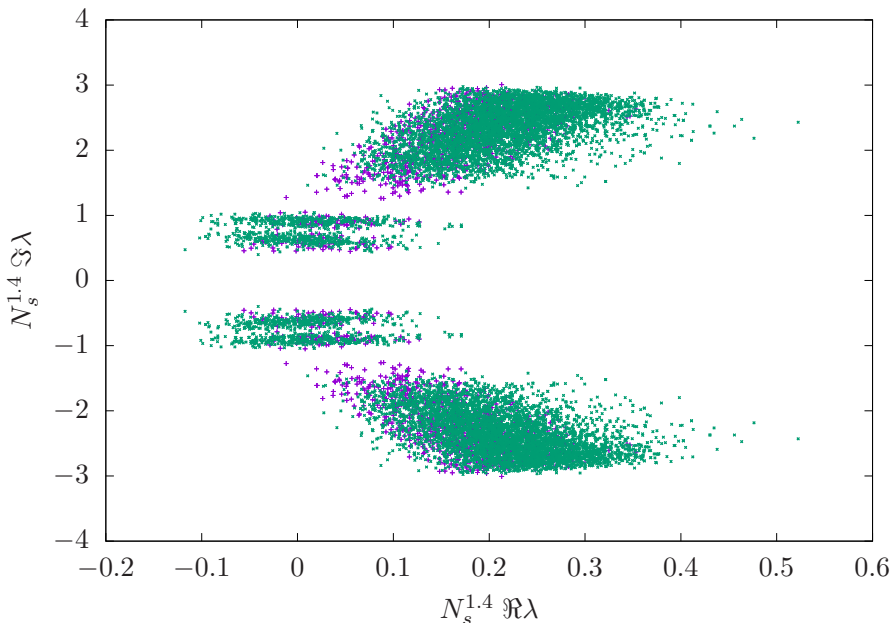


Figure 2: The eigenvalues of the Wilson-Dirac operator for the near-critical runs R1 ($N_s = 24$) and R3 ($N_s = 32$), represented in the complex plane. The smallest eigenvalues in a region around the real axis are determined. We observe a good agreement between the two runs by rescaling the eigenvalues with $N_s^{1.4}$. This scaling of the eigenvalues is in accordance with the scaling by $1 + \gamma^*$ investigated in [11], assuming $\gamma^* \approx 0.4$.

For generating field configurations on the lattice we have used the two-step polynomial hybrid Monte Carlo (PHMC) algorithm [12]. It is based on polynomial approximations of the inverse powers of the Wilson-Dirac matrix. The first polynomial gives a rough

approximation that is corrected by the second polynomial. The polynomials were chosen such that the lower bound of the approximation interval was about a factor 10 smaller than the smallest occurring eigenvalues. The resulting two-step approximation is so good that no further correction by a reweighting factor is necessary in practice.

3 Model parameters and continuum limit

In an asymptotically free gauge theory the lattice spacing a mainly depends on the gauge coupling β . For increasing β the lattice spacing decreases exponentially. The size of a in physical units can be fixed in terms of a dimensionful quantity like the Sommer scale r_0 or the string tension σ , which is used to set the scale.

In an IR conformal theory the situation is different. In the close vicinity of the fixed point the coupling β is an irrelevant parameter and the model depends only weakly on it. Due to the absence of a mass scale the size of the lattice spacing can only be compared to the physical extent $L = N_s a$ of the lattice, and the continuum limit has to be defined in terms of the ratio a/L .

Nevertheless, away from the IR fixed point towards the Gaussian fixed point at $g^2 = 0$ a relevant dependence on β is expected. The theory is asymptotically free in the ultraviolet, and the continuum limit would be reached by sending β to infinity. Near the IR fixed point the dependence on β appears as a correction to scaling.

In addition, the mass term in the action plays an important role. Non-zero masses are relevant parameters that break conformal symmetry and imply corrections to scaling. In the presence of mass terms the renormalisation flow doesn't run into the IR fixed point, but may pass close by. The running of β is then expected to be rather slow.

The dependence of particle masses on the renormalised fermion mass m_r would be quite different for theories in the different scenarios. In a theory above the conformal window, with confinement and chiral symmetry breaking, the mass of the pseudo-Goldstone boson vanishes when the fermion mass m_r goes to zero, whereas the other particle masses approach a finite value, see Fig. 3.

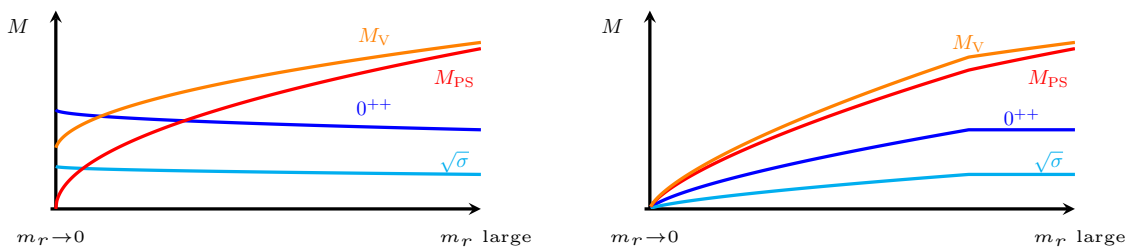


Figure 3: Sketch of the mass spectrum as a function of the fermion mass m_r for a QCD-like (left) and a IR conformal (right) scenario. Indicated are the masses of the pseudoscalar (PS) and vector (V) mesons, the scalar (0^{++}) glueball and the square-root of the string tension σ .

In the IR conformal scenario all particle masses and the string tension would asymptotically scale to zero in the conformal limit according to

$$M \propto m_r^{1/(1+\gamma^*)}, \quad (7)$$

where γ^* is the value of the mass anomalous dimension at the fixed point [13, 14].

In this scenario the ratios of masses are approximately constant for small m_r . These ratios represent universal features of (near) IR conformal theories [15].

In practice, however, the limit of vanishing fermion mass m_r cannot be reached in numerical simulations. In a near conformal theory severe finite size effects would occur for small m_r , and have a substantial influence on the mass spectrum. Moreover, the simulation algorithms slow down strongly at small fermion masses and in this way limit the accessible parameter range.

In our simulations we have chosen two values of $\beta = 1.5$ and 1.7 . We checked that these inverse gauge couplings are above the value of the bulk (“finite temperature”) phase transition. In order to control finite volume effects, lattices of size $16^3 \times 32$, $24^3 \times 48$ and $32^3 \times 64$ have been used for both values of β .

The renormalised fermion mass has been varied by a series of values for the hopping parameter κ . As renormalised fermion mass m_r we take the PCAC mass m_{PCAC} , determined by means of the PCAC (partially conserved axial current) relation. The lattice sizes and parameters for the ensembles with positive fermion mass are summarised in Tab. 1.

The mass of the pseudoscalar meson in lattice units was in the range 0.13 to 1.0. Most relevant for finite size effects are the lightest particle masses, which in our simulations turned out to be the scalar glueball and the pseudoscalar meson. As the mass of the pseudoscalar meson can be determined much easier and precisely, we consider this one as a measure for the low mass scale.

Our results for the various masses show that at $\beta = 1.5$ ensemble A, and at $\beta = 1.7$ ensembles J and K have sizeable finite size effects, so that these ensembles are usually discarded in the analysis, apart from the cases where finite size scaling effects are included.

4 Scaling of the lightest particle masses

The spectrum of colour neutral particles in this model consists of bound states of gauge bosons (“gluons”) and fermions. In addition to mesonic particles and glueballs, spin 1/2 bound states of gluons and fermions are possible due to the adjoint representation of the fermions. In the mesonic sector we consider the scalar and pseudoscalar ones, created by the operators $\bar{\psi}\sigma^a\psi$ and $\bar{\psi}\gamma_5\sigma^a\psi$, $a = 1, 2, 3$, respectively, and the vector and pseudovector mesons, created by $\bar{\psi}^b\gamma_k\psi^c$ and $\bar{\psi}^b\gamma_5\gamma_k\psi^c$, respectively, where $k = 1, 2, 3$ is in the spatial direction. In addition, the scalar glueball and the spin 1/2 fermion-gluon bound state, represented by $\sigma_{\mu\nu}\text{tr}[F^{\mu\nu}\psi]$, have been investigated. Apart from the particle masses we have also calculated the string tension σ from the static quark-antiquark potential, where “quark” means a particle in the fundamental representation

	β	N_s	κ	am_{PCAC}
A	1.5	16	0.137	0.02270(18)
B	1.5	16	0.135	0.11604(44)
C	1.5	16	0.132	0.23236(83)
D	1.5	24	0.1351	0.10986(12)
E	1.5	24	0.134	0.15632(15)
F	1.5	24	0.133	0.19515(20)
G	1.5	24	0.132	0.23207(22)
H	1.5	32	0.1359	0.07380(07)
J	1.7	16	0.130	0.12890(77)
K	1.7	24	0.133	0.03360(30)
L	1.7	24	0.132	0.06628(08)
M	1.7	24	0.130	0.12882(15)
N	1.7	32	0.132	0.06635(12)
O	1.7	32	0.130	0.12910(04)
P	1.7	32	0.1285	0.17366(04)
Q	1.7	48	0.1322	0.05990(05)
R1	1.7	24	0.134	-0.00097(22)
R3	1.7	32	0.134	-0.00052(11)

Table 1: Parameters of the simulation ensembles.

of the colour gauge group. The square-root of σ has dimensions of a mass and scales as a mass. Therefore we include it in our analysis of the scaling behaviour. The techniques for the calculation of the propagators, masses and string tension have been explicated in [4] and for details we refer to this article.

Fig. 4 shows the particle masses as a function of the fermion mass. All masses appear to scale downwards towards the limit $m_{\text{PCAC}} = 0$. The lightest particle, being well separated from the rest, is the scalar glueball. So the overall behaviour indicates a scenario different from the QCD-like one, where the pseudoscalar pseudo-Goldstone boson is lightest particle. As expected for a theory in the conformal window, all masses scale approximately in the same way and their ratios are constant as shown in Fig. 5.

In order to substantiate this impression we have investigated the scaling behaviour of masses. To begin with, consider the pseudoscalar meson. In a QCD-like situation this particle is the pseudo-Goldstone boson of spontaneously broken chiral symmetry, and its mass vanishes with $m_r \equiv m_{\text{PCAC}}$ according to the Gell-Mann-Oakes-Renner relation $m_{\text{PS}} \propto m_r^{1/2}$. On the other hand, in an IR-conformal scenario m_{PS} would scale to zero as $m_{\text{PS}} \propto m_r^k$ with an exponent $k = 1/(1 + \gamma^*)$ that can be different from 1/2. In order to determine the exponent k we fitted $\ln(m_{\text{PS}})$ as a linear function of $\ln(m_r)$. As mentioned above, ensembles A, K and J are omitted in view of finite size effects. Being even more restrictive concerning possible finite size effects, one would also leave out the ensembles N, L and Q with the smallest fermion masses at $\beta = 1.7$, remaining with M, O, P.

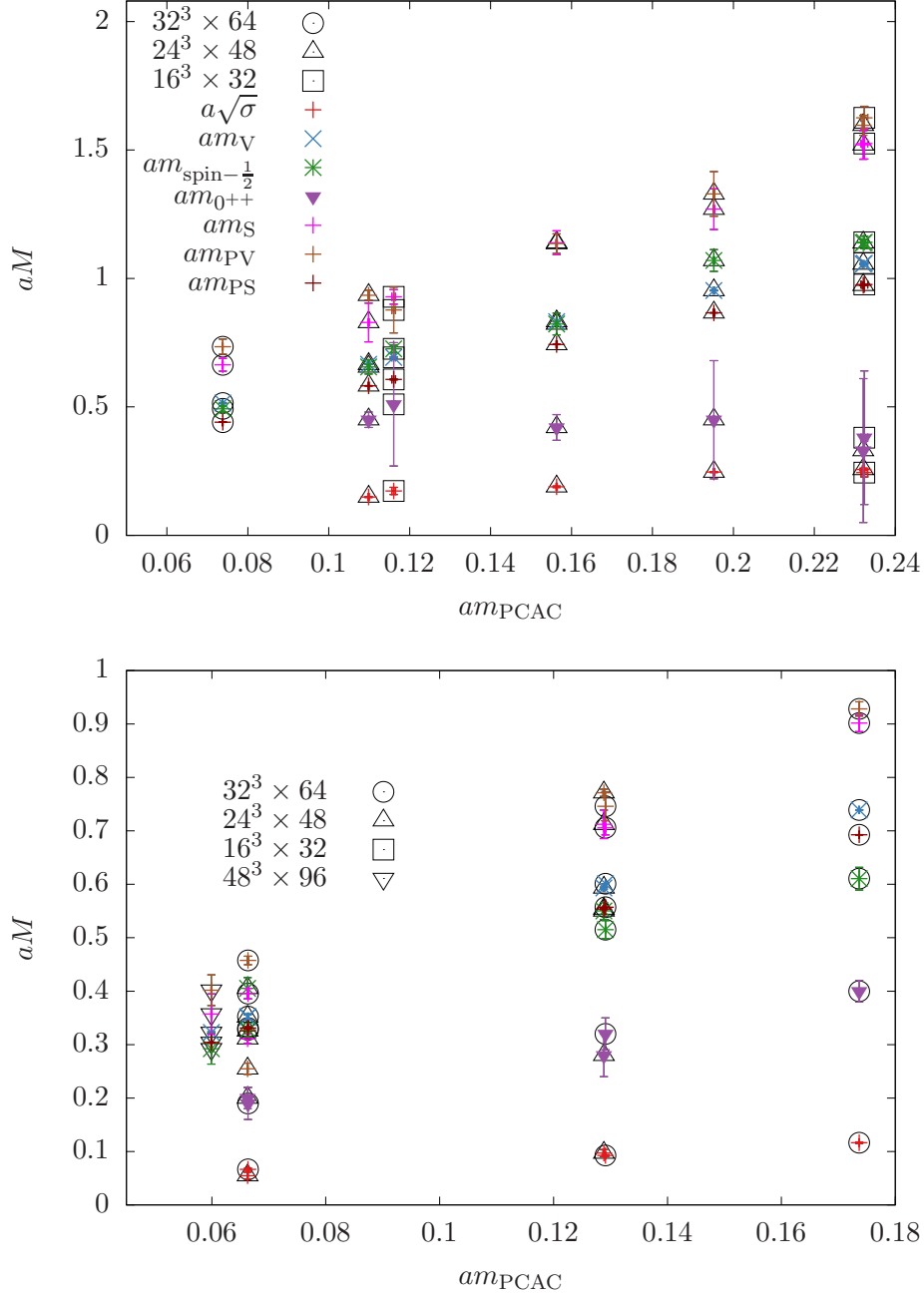


Figure 4: Particle masses and $\sqrt{\sigma}$ as a function of am_{PCAC} for $\beta = 1.5$ (above) and $\beta = 1.7$ (below).

The data points show a nice linear behaviour. For $\beta = 1.5$ the fit gives an exponent $k = 0.691(2)$, and for $\beta = 1.7$ we obtain $k = 0.743(14)$ from ensembles (M, O, P). An estimate of the systematic error is obtained by considering different subsets of ensembles. For $\beta = 1.7$ we get $k = 0.775(8)$ from the $N_s = 32, 48$ lattices (N, O, P, Q), and $k = 0.780(7)$ from ensembles L – Q. Thus the exponent is evidently different from 0.5,

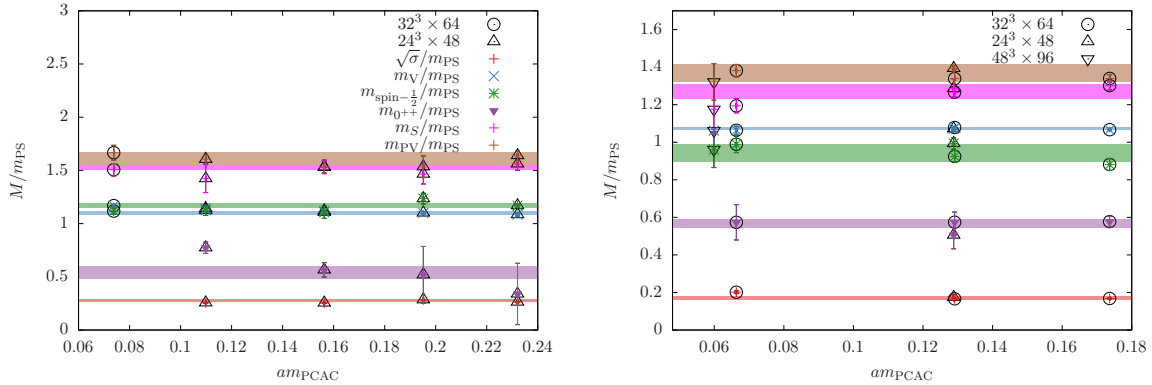


Figure 5: Particle masses and $\sqrt{\sigma}$ in units of the pseudoscalar mass as a function of am_{PCAC} for $\beta = 1.5$ and $\beta = 1.7$.

indicating the IR-conformal scenario. In this case, the other masses should show scaling with the same exponent. We considered the weighted average of the logarithms of the other masses $m_S, m_V, m_{PV}, m_{0^{++}}, m_{1/2}$ and $m_\sigma = \sqrt{\sigma}$, the weights given by the inverse variances as usual, as a function of $\ln(m_r)$. Again a nice linear behaviour can be seen. From the linear fit we obtain $k = 0.608(17)$ for $\beta = 1.5$ and $k = 0.667(54)$ for $\beta = 1.7$, ensembles M, O, P. These values are compatible with the ones from m_{PS} and give clear support for the IR-conformal scenario.

The overall estimate of the mass anomalous dimension is obtained by the same fit, now including the pseudoscalar mass. For $\beta = 1.5$ this gives $k = 0.675(24)$. The corresponding number for $\beta = 1.7$, ensembles M, O, P, is $k = 0.751(8)$. For comparison, we get $k = 0.817(36)$ from N, O, P, Q, and $k = 0.817(24)$ from L – P. Fig. 6 shows the averaged logarithmic masses for $\beta = 1.7$ and the fit with $k = 0.751$.

To conclude, the particle masses show scaling behaviour of the IR-conformal scenario with an exponent $k \approx 0.67$, corresponding to $\gamma^* \approx 0.5$, for $\beta = 1.5$, and $k = 0.75(7)$, corresponding to $\gamma^* = 0.33(13)$, for $\beta = 1.7$.

5 Mode number

An alternative method for the determination of the mass anomalous dimension is based on the spectral density of the Dirac operator [16, 17, 18, 19, 20]. The mode number $\nu(\Omega)$ is defined to be the number of eigenvalues of the hermitian operator $D_w^\dagger D_w$ below some limit Ω^2 . The mode number obeys a scaling law [17]

$$\nu(\Omega) = \nu_0 + a_1(\Omega^2 - a_2^2)^{2/(1+\gamma^*)} \quad (8)$$

for sufficiently small values of $\Omega^2 - a_2^2$, where a_2 is proportional to m_{PCAC} . Therefore, a fit of $\nu(\Omega)$ to this function in a suitable range $[\Omega_{\text{min}}, \Omega_{\text{max}}]$ allows to estimate the mass anomalous dimension γ^* .

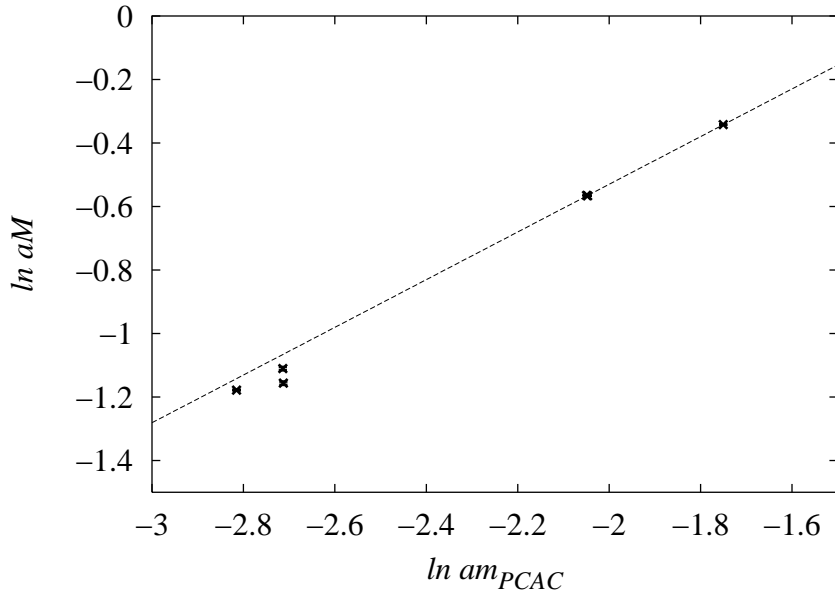


Figure 6: Weighted averages of the logarithms of the particle masses at $\beta = 1.7$ as a function of $\ln(am_{PCAC})$, and the scaling fit with exponent $k = 0.751$. Note that the second symbol from right stands for two close-by data points and the three leftmost points are not included in this fit.

The choice of the fit range $[\Omega_{\min}, \Omega_{\max}]$ is a sensitive issue. For a small fit range near a scale Ω , the resulting value for the mass anomalous dimension can be considered as an effective anomalous dimension $\gamma(\Omega)$, which approximates the corresponding renormalisation group function [18]. For large Ω it is expected that $\gamma(\Omega)$ decreases and approaches its value zero at the asymptotically free UV fixed point. On the other hand, for small Ω finite volume effects and effects of the non-vanishing fermion mass m_{PCAC} will disturb the scaling behaviour. Therefore the fit range should be located in an intermediate regime, where the effects of the finite volume and non-zero fermion mass can be neglected [17, 20]. For an infrared conformal theory the coupling runs very slowly for a wide range of scales at low μ , and there the anomalous dimension γ varies slowly, too, approximatively developing a plateau at the value γ^* . Investigations of the β -function in the MiniMOM scheme for this theory [21] indicate that the $N_f = 3/2$ theory appears to be close to the the edge of the conformal window.

The techniques and the code that we have implemented to compute the mode number have been tested in the $N_f = 2$ case and presented in Ref. [9]. We have used different methods for the non-linear fit to Eq. 8 including parallel tempering together with conjugate gradient techniques. The fit of a large number of data points requires particular techniques for the determination of the correlated χ^2 [22]. The results for the fits over intervals of fixed length and varying lower end Ω_{\min} are shown in Figs. 7 and 8 for the runs at $\beta = 1.5$ and $\beta = 1.7$, respectively.

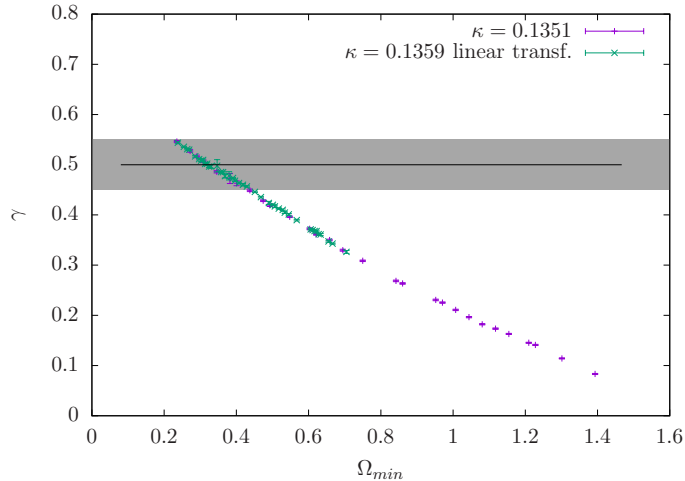


Figure 7: Fitted value of the mass anomalous dimension for the ensemble at $\beta = 1.5$, $\kappa = 0.1351$ (ensemble D), and $\kappa = 0.1359$ (ensemble H). Ω_{\min} denotes the lower end of the fitting interval, while the upper end is fixed to $\Omega_{\min} + 0.07$. The Ω_{\min} values on the x-axis are rescaled by the linear transformation $\Omega'_{\min} = 0.88\Omega_{\min} + 0.1$ for $\kappa = 0.1359$ in order to collapse the two ensembles. In the shaded region we obtain the best fits for both ensembles. Fits with a correlated χ^2 per degree of freedom larger than 4 are excluded.

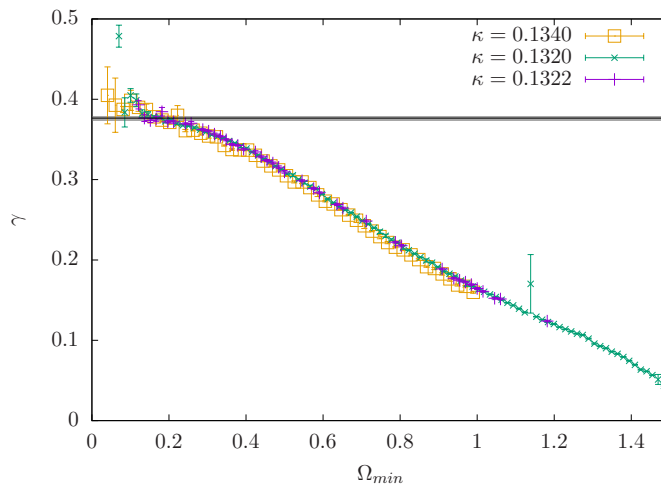


Figure 8: Fitted value of the mass anomalous dimension for the ensemble at $\beta = 1.7$, $\kappa = 0.1322$ (ensemble Q), $\kappa = 0.1320$ (ensemble N), and $\kappa = 0.1340$ (ensemble R3), as in Figure 7. Ensembles N and R3 are only shown for comparison. Fits of the data from ensemble Q with a correlated χ^2 per degree of freedom larger than 4 have been excluded from the figure. The final value represented by the shaded region in the plot is only obtained from a fit in the plateau region of ensemble Q.

At $\beta = 1.5$ we obtain reasonable fits with an acceptable p-value and a correlated χ^2 per degree of freedom in a certain region of Ω values for the ensembles with the smallest fermion masses. However, there is no pronounced plateau for the obtained values in this range. The best fits are obtained at rather large values of Ω . Further in the infrared, the correlated χ^2 of the fit drastically increases, which is an indication of fermion mass effects. We take the final value from the middle of the range where the correlated χ^2 per degree of freedom is below 2.5 for ensemble H, and the width of this range as an estimate for the error. This provides a rough estimate of $\gamma^* \approx 0.5 \pm 0.05$.

In contrast to the case of $\beta = 1.5$, a considerable plateau of the fitted values is obtained at $\beta = 1.7$ in the infrared region. The plots of the fit results agree in a large range of Ω_{\min} values for the ensembles Q and N. Hence they are quite insensitive to a change of the fermion mass and the volume. Even the plot for ensemble R3, at approximate zero fermion mass, agrees with these data. Due to the uncertainties originating from the polynomial choices in the PHMC algorithm at ensemble R3, we have only considered ensemble Q for the final fit. We obtain a value of $\gamma^* \approx 0.377(3)$. Taking also the uncertainties in the determination of the fitting interval into account, the estimate is $\gamma^* \approx 0.38(2)$.

We made a crosscheck of the obtained values of γ^* with the hyperscaling of the mass spectrum. As shown in Fig. 9, the agreement with the expected functional behaviour is reasonable. We can also vary the exponents close to the measured values in order to minimise the sum of the χ^2 from the linear fits. In this way we obtain a minimum around $\gamma^* \approx 0.46(2)$ for $\beta = 1.5$ and $\gamma^* \approx 0.37(2)$ for $\beta = 1.7$. This shows that the values for the mass anomalous dimension obtained from the mode number are consistent with the hyperscaling of the mass spectrum

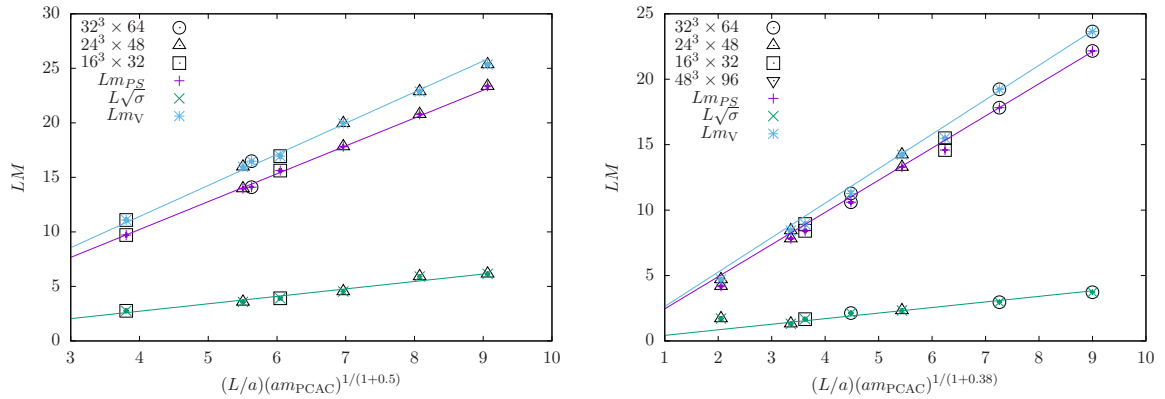


Figure 9: A cross check of the scaling exponents obtained from the mode number with the scaling of the particle masses. These figures show a fit to the hyperscaling hypothesis of the masses including volume scaling. The points with the smallest values on the x-axis correspond to the ensembles B ($\beta = 1.5$) and K ($\beta = 1.7$). The lines correspond to a linear fit, in case of $\beta = 1.7$ without the data of ensemble K.

6 Conclusions

We have analysed the spectrum of bound states masses in $SU(2)$ gauge theory with $N_f = 3/2$ flavours of adjoint fermions at two values of the inverse gauge coupling $\beta = 1.5$ and 1.7 . The scaling of the masses as a function of the fermion mass m_{PCAC} indicates an infrared conformal behaviour of this theory. The fixed point value of the mass anomalous dimension is estimated to be $\gamma^* \approx 0.5$, for $\beta = 1.5$, and $\gamma^* = 0.33(13)$, for $\beta = 1.7$. An independent estimate has been obtained from the scaling of the mode number of the hermitian Wilson-Dirac operator. For $\beta = 1.5$ we only get a rough estimate of $\gamma^* \approx 0.5$, whereas for $\beta = 1.7$ a plateau shows up at a value of $\gamma^* \approx 0.38(2)$.

For a conformally behaving theory in the infinite volume limit the value of γ^* should be independent of the gauge coupling. On the other hand, for a theory in the vicinity of an IR fixed point, scaling violations are present, which increase towards the UV regime. The fact that our estimates at the two gauge couplings do not exactly coincide indicates the influence of scaling violations and cutoff effects.

Acknowledgments

The authors gratefully acknowledge the Gauss Centre for Supercomputing (GCS) for providing computing time for a GCS Large-Scale Project on the GCS share of the supercomputer JUQUEEN at Jülich Supercomputing Centre (JSC) and on the supercomputer SuperMUC at Leibniz Computing Centre (LRZ). GCS is the alliance of the three national supercomputing centres HLRS (Universität Stuttgart), JSC (Forschungszentrum Jülich), and LRZ (Bayerische Akademie der Wissenschaften), funded by the German Federal Ministry of Education and Research (BMBF) and the German State Ministries for Research of Baden-Württemberg (MWK), Bayern (StMWFK) and Nordrhein-Westfalen (MIWF). Further computing time has been provided by the compute cluster PALMA of the University of Münster.

References

- [1] T. Banks and A. Zaks, Nucl. Phys. B **196** (1982) 189.
- [2] B. Holdom, Phys. Rev. D **24** (1981) 1441.
- [3] D. D. Dietrich and F. Sannino, Phys. Rev. D **75** (2007) 085018 [arXiv: hep-ph/0611341].
- [4] G. Bergner, P. Giudice, G. Münster, I. Montvay and S. Piemonte, Phys. Rev. D **96** (2017) 034504 [arXiv: 1610.01576 [hep-lat]].
- [5] T. DeGrand, Rev. Mod. Phys. **88** (2016) 015001 [arXiv: 1510.05018 [hep-ph]].
- [6] C. Pica, PoS(LATTICE2016) 015 [arXiv: 1701.07782 [hep-lat]].

- [7] A. Athenodorou, E. Bennett, G. Bergner and B. Lucini, Phys. Rev. D **91** (2015) 114508 [arXiv:1412.5994 [hep-lat]].
- [8] G. Bergner, P. Giudice, G. Münster, I. Montvay and S. Piemonte, JHEP **1603** (2016) 080 [arXiv:1512.07014 [hep-lat]].
- [9] G. Bergner, P. Giudice, I. Montvay, G. Münster and S. Piemonte, PoS(LATTICE2016) 237 [arXiv:1701.08992 [hep-lat]].
- [10] C. Morningstar and M. J. Peardon, Phys. Rev. D **69** (2004) 054501 [arXiv:hep-lat/0311018].
- [11] N. Karthik and R. Narayanan, Phys. Rev. D **94** (2016) 065026 [arXiv:1606.04109 [hep-th]].
- [12] I. Montvay and E. Scholz, Phys. Lett. B **623** (2005) 73 [arXiv:hep-lat/0506006].
- [13] M. A. Luty, JHEP **0904** (2009) 050 [arXiv:0806.1235 [hep-ph]].
- [14] L. Del Debbio and R. Zwicky, Phys. Rev. D **82** (2010) 014502 [arXiv:1005.2371 [hep-ph]].
- [15] A. Athenodorou, E. Bennett, G. Bergner, D. Elander, C.-J. D. Lin, B. Lucini and M. Piai, JHEP **1606** (2016) 114 [arXiv:1605.04258 [hep-th]].
- [16] L. Giusti and M. Lüscher, JHEP **0903** (2009) 013 [arXiv:0812.3638 [hep-lat]].
- [17] A. Patella, Phys. Rev. D **86** (2012) 025006 [arXiv:1204.4432 [hep-lat]].
- [18] A. Cheng, A. Hasenfratz, G. Petropoulos and D. Schaich, PoS(LATTICE 2013) 088 [arXiv:1311.1287 [hep-lat]].
- [19] Z. Fodor, K. Holland, J. Kuti, D. Nógrádi and C. H. Wong, PoS(LATTICE 2013) 089 [arXiv:1402.6029 [hep-lat]].
- [20] K. Cichy, JHEP **1408** (2014) 127 [arXiv:1311.3572 [hep-lat]].
- [21] G. Bergner and S. Piemonte, [arXiv:1709.07367 [hep-lat]].
- [22] C. Michael and A. McKerrell, Phys. Rev. D **51** (1995) 3745 [arXiv:hep-lat/9412087].